OPTICAL DETECTION OF DIFFERENT PHENOLIC COMPOUNDS BY MEANS OF A NOVEL BIOSENSOR BASED ON SOL-GEL IMMOBILIZED LACCASE

Running Title: **Optical detection of phenolic compounds**

Maria Lepore*, Marianna Portaccio

Dipartimento di Medicina Sperimentale

Seconda Università di Napoli, Via S.M. di Costantinopoli, 16-80134 Napoli, Italy

* Corresponding author: Tel: +39 081 5667539; E-mail address: maria.lepore@unina2.it

This article has been accepted for publication and undergone full peer review but has not been through the copyediting, typesetting, pagination and proofreading process, which may lead to differences between this version and the Version of Record. Please cite this article as doi: 10.1002/bab.1551.

ABSTRACT

A novel sol-gel based biosensor exploiting the optical absorption properties of sol-gel immobilized laccase has been constructed in the attempt to increase enzyme specificity towards different phenolic substrates. Laccase from *Trametes versicolor* has been immobilized in optically transparent sol-gel matrices. Using Fourier transform infrared spectroscopy and data analysis based on a wavelet algorithm the successful enzyme immobilization has been evidenced. The changes in the optical absorption spectra of laccase reaction products at 425 nm, 375 nm and 400 nm have been used for hydroquinone, resorcinol and catechol concentration determination, respectively. Due to the slow response time of hydroquinone-laccase reaction, our optical biosensor has been tested with resorcinol and catechol. Linear ranges up to 1.4 mM and 0.2 mM, limit-of-detection (LOD) of 4.5 μM and 0.6 μM have been evidenced for resorcinol and catechol, respectively. Data for resorcinol concentration determination have been particularly interesting since no other biosensor device has been reported in literature. In comparison with other biosensors using laccase from the same native source our biosensor has been characterized by larger linear ranges, significant sensitivities and good LODs. To challenge our biosensor with real samples, tap water samples spiked with known amount of catechol and resorcinol have been employed.

Keywords: catechol; hydroquinone; laccase; optical biosensors; resorcinol; silica gel.

1. Introduction

Water is one of the most important environmental compounds and the attention to the problems related to the water environment and its pollution has become of considerable interest in recent years. Among the potentially hazardous substances to the water, there are phenolic compounds that are used in many industrial processes, such as the production of pesticides, insecticides, herbicides and synthetic products and are found in industrial wastewater. They are toxic compounds that can produce poisoning by absorption through the skin, ingestion or inhalation of vapours [1]. Methods to determine phenols at a very low concentration are gas chromatographic (GC), flame ionic detection (FID) or derivatization and electron capture detection (ECD). Other methods to determine phenols at slightly higher concentrations are liquid–liquid extraction gas chromatographic/mass spectrometric method [2]. However these techniques are very demanding in terms of time, costs and they do not allow in situ measurements, therefore there is a considerable interest in the development of easy-to-use, highly sensitive and with good specificity biosensors. In this framework, laccases can play a relevant role. Laccases (benzenediol oxygen oxidoreductase, EC 1.10.3.2) are cuproproteins and belong to a small number of enzymes called polyphenol oxidase or blue multicopper [3, 4]. Most of laccases contains four copper atoms per functional unit, which are essential for catalytic activity. The copper atoms are distributed in different binding sites and they are classified into three types according to the specific spectroscopic characteristics, functional and paramagnetic properties. The copper of type 1 (T1) absorbs electromagnetic radiation around 600 nm and it is responsible for the characteristic blue colour of these cuproproteins. It's presumably the primary site of oxidation. Copper Type 2 (T2) shows only a weak absorption in the visible but is EPR active. The two copper atoms of type 3 (T3) are characterized by an absorption band around 330 nm and are EPR silent [5, 6]. Laccases catalyze the oxidation of various aromatic compounds, such as ortho and para diphenols, polyphenols, aminophenols and aromatic amines, with the concomitant reduction of molecular oxygen to water [7]. From literature it's evident that laccases have been mainly employed for the design and fabrication of electrochemical biosensors for the detection of phenol compounds [8-15] with significant linear ranges, sensitivity and detection limit (see Table 1 in ref. 11). As far as concerns optical biosensors few of them have been reported in literature notwithstanding the significant optical properties of laccases [16-19] and the experimental evidence that optical biosensors have been generally characterized by a high sensitivity [20]. Some of the optical laccase biosensors reported in literature have used fluorescence measurements and the unique physicochemical properties of nanoparticles and quantum dots have been also successfully exploited to improve the linear range, sensitivity and selectivity [21, 22]. An optical laccase biosensor for detection of phenolic compounds has been developed by Abdullah et al. [23]. The optical biosensor has been prepared by using chitosan-laccase solution and stacked films where 3-methyl- 2-benzothiazolinone hydrazone (MBTH) immobilized in a hybrid nafion/sol-gel silicate film. Quinone and/or phenoxy radical product from the enzymatic oxidation of phenolic compounds has been allowed to

couple with MBTH to form a coloured azo-dye product for spectrophotometric detection. Another optical biosensing scheme has been proposed by Sanz et al [24] exploiting absorption properties for phenol detection using polyacrylamide film for laccase immobilization. Laccases and phenol reaction products present significant optical characteristics in UV and visible range that until now have been mainly adopted for developing spectrophotometric methods for measuring laccase activity [25-28]. Similar methods can be suitably modified for biosensing applications taking into account that laccase interacting with different phenols shows absorption spectra with different spectral characteristics. These differences can improve the specificity of laccase-based biosensors that is generally considered rather low [29]. In order to develop optical biosensors able to exploits the above mentioned spectral features optically transparent matrices for enzyme immobilization are required. Sol-gel technology can be extremely useful for fabricating optical biosensing elements owing to superior chemical stability, optical transparency and porosity of sol-gel matrices. [30-35].

Sol-gel matrices with immobilized laccase from *Trametes versicolor* have been used for designing a new biosensor based on the changes in the optical absorption due to the interaction of the immobilized laccase with different phenol compounds. In particular hydroquinone, resorcinol and catechol have been investigated and the linear range, the sensitivity and the limit of detection (LOD) have been measured. The proposed biosensor has been tested with real samples using tap water spiked with known amount of catechol and resorcinol. It's worth to note that no other biosensing device for resorcinol concentration determination has been reported in literature to our knowledge.

2. Materials and Methods

2.1 Materials

All chemicals and commercial laccase were purchased from Sigma (Sigma Italia, Milan, Italy), with the exception of tetramethoxysilane (TMOS) and methyl-trimethoxysilane (MTMOS) which were purchased from Fluka (Fluka Italia, Milan, Italy). In this study laccase from *Trametes versicolor* with an enzymatic activity equal to 20 U/mg was used without any further purification. Free laccase solutions with a concentration equal to 8 μg/mL were obtained by using 0.1 M acetate buffer at pH 5. Hydroquinone, resorcinol and catechol were dissolved in the same buffer at different concentrations as required by experiments.

2.2 Methods

2.2.1 Preparation of catalytic sol–gel matrices

Silica gel matrices were prepared by rapid mixing of 600 μL of solution A with 600 μL of solution B by modifying a previously reported preparation procedure [33]. Solution A was obtained by slowly mixing (for 1 h at 4 °C) 1200 μL of TMOS + 400 μL of MTMOS solution, plus 480μL of H_2O and 48μL of 40 mM HCl. Solution B contained 0.1 M phosphate buffer at pH 6.5. The A and B solution mixture (1200 μL) was poured into a polymethylmethacrylate cuvette that was after sealed. To avoid cracking once the gel was formed, after a first step of gelification (about 15 min) the cuvette was filled with 0.1 M phosphate buffer at pH 6.5 and stored overnight in a refrigerator at 4 °C. The day after, the silica gel layer was removed from the cuvette and was ready for use. The catalytic gel was prepared with solution B containing an additional 5 mg/mL of laccase. For spectrophotometric measurement sol-gel sample were prepared with 8x30x3 mm size. When not used, the sol-gel layers were stored at 4 °C in buffer solution pH 5.0 and showed good storage stability over a period of 60 days.

It is important to note that the hydrophobic organic ligands of silane precursors are important for defining the characteristics of gel matrices, that are fundamental for the catalytic properties of laccase preparation and its interaction with hydrophobic substrate [36]. For this reason MTMOS compound was added in solution A to increase the sol-gel hydrophobicity. In Fig. 1 a representative scheme of catalytic sol-gel preparation is reported.

2.2.2 FT-IR spectroscopy

A Perkin Elmer Spectrum One FT-IR spectrometer equipped with a MIR TGS detector was used to record FT-IR spectra. The samples were examined by using KBr pellets. Before collection, background scanning was performed using empty KBr pellets. All spectra were collected using 16 scans in the range from 4.000 to 600 cm^{-1} with a 4 cm^{-1} spectral resolution. Each sample was investigated in triplicate. The spectra were preliminarily analyzed using the application routines provided by the software package ("Spectrum" User Guide, Perkin Elmer Inc. USA) controlling the whole data acquisition system. "Spectrum" is the main Perkin Elmer software package for collecting, viewing and processing IR spectra.

FT-IR spectroscopy is a technique largely employed for support characterization and for confirming the successful enzyme immobilization [34-35]. In order to evidence differences between infrared spectra related to different samples a data analysis procedure successfully applied in Raman spectra analysis was adopted here. In particular, an automatic numerical treatment based on wavelet algorithm was used [37 and references therein]. The infrared spectrum was assimilated to a time modulated signal f(t) on a finite interval, where the wavenumber shift stood as the variable t. The wavelet algorithm cut up the signal into different "frequency" components, similarly to the conventional Fourier transform, but it used spatially localized functions with average zero value (namely wavelets, small waves),

instead of conventional sinusoidal functions, allowing to obtain information on both frequency and time dependence. MATLAB 6.5 program (by MathWorks Inc., Natick, MA, USA) was used for wavelet analysis.

2.2.3 Absorption and time course measurements

All the absorption measurements were performed using a Lambda 25 Perkin Elmer (Perkin-Elmer Italia, Milano, Italy) spectrophotometer working in the 200-900 nm range.

UV-VIS spectra were obtained for laccase, phenols compounds before and after laccase interaction using a quartz cuvette. In the case of sol-gel matrix samples with and without laccase enzyme the gel layers were placed in the same cuvette filled with 3 mL 0.1 M acetate buffer solution at pH 5.

For bioanalytical applications time course measurements of changes in the absorption were performed using the same spectrophotometer. These measurements were performed at an optimized fixed wavelength experimentally determined by monitoring the enzymatic reaction between laccase and the phenol compound. At the beginning, the absorption of either free or immobilized laccase at the optimized fixed wavelength was measured. This measure constitutes the baseline for the subsequent measurements. After addition of few μliters of solution of different phenols at various concentrations the time course of the absorption intensity was monitored and absorption changes for unit of time were determined.

All measurements were performed at 20 °C and each sample was examined in triplicate.

3. Results and Discussion

3.1 FT-IR spectroscopy

In order to monitor the laccase immobilization in the sol-gel matrix FT-IR spectroscopy was used. A representative FT-IR spectrum of laccase is reported in Fig. 2a in which some typical characteristics of infrared protein spectra are present. In particular, a large contribution from amide A and OH groups is evident at 3401 cm^{-1}, the small peak at 2922 cm^{-1} can be due to CH symmetric stretching in CH_2. The peaks at 1647 cm^{-1} and 1545 cm^{-1} can be assigned to amide I and amide II contribution, respectively. As said before FT-IR

spectroscopy can been used to monitor the enzyme immobilization and these two peaks are usually chosen for evidencing successfully enzyme immobilization [33, 34 and references therein]. The peaks at 1408 cm^{-1} can be ascribed to C–H bending of CH_3 group; the peak at 1250 cm^{-1} is due to amide III contribution, the band at 1036 cm^{-1} is ascribed to C-O stretching and the small peak at 804 cm^{-1} can be due to amide V contribution. For a complete assignment according to refs. 34 and 38 please refer to Table 1. In Fig. 2b a representative FT-IR spectrum (dashed line) of a sol-gel matrix is reported. The large band at 3495 cm^{-1} can be ascribed to H-bonded silanol and O–H stretching, the small peaks at 2919 cm^{-1} and 2850 cm^{-1} are generally associated with CH asymmetric stretching in $O–CH_3$ and CH symmetric stretching in $O–CH_3$ contribution, respectively. In this case the peak at 1645 cm^{-1} can be due to H-bonded silanol and O–H bending. The peak at 1280 cm^{-1} can be due to Si-CH_3 and symmetric CH_3 deformation vibration, the large asymmetric band at 1057 cm^{-1} is characteristics of the silica sol-gel materials and is due to Si–O–Si asymmetric stretching, the peak at 951 cm^{-1} can be associated with Si–OH deformation vibration and the one at 799 cm^{-1} can be related to Si–O–Si symmetric stretching. For a complete assignment according to refs. 34 and 38-40 please refer to Table 2. In Fig. 2b also the FT-IR spectrum (continuous line) of a sol-gel immobilized laccase sample is reported. As can see the two spectra are largely similar with the exclusion of small wavenumber shifts of some peaks and the presence of two small contributions at 1552 cm^{-1} and 1414 cm^{-1} that can be related to amide II and C–H bending CH_3, respectively. At first glance, there is no clear evidence of laccase presence. In fact using commercial or not extremely purified laccases is not so easy to evidence the occurred immobilization [41]. To evidence the contribution of immobilized enzyme the procedure previously adopted in refs. 34 and 35 for monitoring the glucose oxidase immobilization hasn't given satisfactory results. For this reason the above-mentioned wavelet data analysis has been adopted and has allowed us to obtain reconstructed spectra evidencing that the 1800-1300 cm^{-1} region shows significant differences between the two spectra of Fig. 2b. In particular the spectrum reported in the inset of Fig. 2b has been obtained by subtracting the reconstructed spectrum of the sol-gel matrix with laccase to the reconstructed spectrum of the bare sol-gel matrix. The inset shows the contribution at 1668 cm^{-1}, 1552 cm^{-1} and 1414 cm^{-1} that can be ascribed (within the spectral resolution experimentally available) to amide I, amide II and C–H bending of CH_3 group, respectively. Their presence can confirm that laccase has been successfully immobilized in sol-gel matrix [42, 43] even though Amide I band appears shifted to higher wavenumbers. This evidence can indicate the dominance of a more disordered β-turn component or a possible interaction between sol-gel matrix and laccase [44]. In addition the relative intensity of Amide I and Amide II band is changed in comparison with FT-IR spectrum of native laccase similarly to what observed from Diaconu et al for laccase from *Trametes versicolor* entrapped in a nanocomposite chitosan film [44]. In their paper the presence of Amide I and Amide II band with an intensity ratio in the FT-IR spectrum of immobilized enzyme different from the one present in the spectrum of native enzyme is still assumed to indicate a good functionality. In our case the preservation of enzymatic activity of our catalytic elements is further confirmed by the calibration curves later discussed.

3.2 UV–Vis Spectra Analysis

In Fig. 3a the absorption spectrum of laccase in solution (concentration equal to 1 mg/mL in 0.1 M acetate buffer pH 5) is reported, the contribution of peptide bonds at 230 nm and of tyrosine and tryptophan at 280 nm can be noticed, the contribution of T3 is evidenced around 330 nm by a small enhancement. The T1 contribution can be recognized only in inset of Fig. 3a where more appropriate axis scales are used. The intensity of T3 and T1 contributions is very low in comparison with results reported in refs. 18 and 45, but in these papers enzyme purification procedures have been adopted. Conversely, for our biosensing applications, we have decided to use commercial enzymes without any further manipulation. In Fig. 3b the absorption spectrum (i line) of laccase immobilized in the sol-gel matrix is shown along with the corresponding spectrum (ii line) of bare sol-gel. As evident the sol-gel has a negligible absorption in all the visible range and the contributions of peptide bonds at 220 nm and of tyrosine and tryptophan at 280 nm are detectable when the enzyme is immobilized. The contribution of T3 copper site is negligible. The presence of the 220 nm and 280 nm peaks further confirms the immobilization of laccase.

As well known laccase can catalyze the oxidation of hydroquinone (p-benzenediol), resorcinol (m-benzenediol) and catechol (o-benzenediol) to o,m,p-quinones by oxygen in solution according to the following reaction [14, 46]:

$$o,m,p-benzenedid+\frac{1}{2}O_2 \xrightarrow{laccase} o,m,p-quinone+H_2O \qquad 1)$$

where the oxygen is directly reduced to water without the intermediate formation of hydrogen peroxide. Since these reaction products, i.e., the quinones formed in reaction (1), are electrochemically active, the concentration of phenolic compounds can be determined by monitoring the current of these enzymatic products on the electrode as occur in electrochemical biosensors [7-10]. The reaction (1) can be also optically followed by measuring absorption changes at a well-chosen wavelength (depending on the chosen phenolic compound) as performed in many spectrophotometric assays for laccase activity determination [26-28].

Fig. 4a shows the UV absorption spectrum (dashed line) of hydroquinone and of the product of enzymatic oxidation due to laccase interaction (continuous line). The hydroquinone spectrum is characterized by a peak at 225 nm that is can be mainly attributed to π-π^* electronic transitions centred on aromatic ring while the band at 290 nm may be due to donor-acceptor charge transfer [47, 48]. As far as concerns the absorption spectrum (continuous line) of hydroquinone oxidized by laccase, a new peak appears at 425 nm, which corresponds to the formation of p-benzoquinone (see Fig 4a inset) [48]. During the slow

enzymatic oxidation, the colour of hydroquinone solution changes from colourless to dark wine red.

In Fig. 4b the UV-Vis spectra for resorcinol (dashed line) and resorcinol interacting with laccase (continuous line) are reported. The resorcinol spectrum shows features similar to the ones already discussed for hydroquinone spectrum, with the two bands located at 220 nm and 270 nm. For resorcinol the colour of solution changes from colourless to dark orange during enzymatic oxidation. The peak related to the resorcinol-laccase interaction is present at 375 nm as shown by Fig.4b inset [49].

In Fig. 4c the UV-Vis spectra for catechol (dashed line) and catechol interacting with laccase (continuous line) are reported. For catechol the two bands are located at 220 nm and 275 nm and the colour of solution changes from colourless to dark brown during enzymatic oxidation. A peak related to the catechol-laccase interaction is present at 400 nm [50-51] as shown by Fig. 4c inset. It must be noted that the here reported absorption spectra for laccase interacting with various phenols show maximum located at a different wavelength. This could be exploited for preparing optical biosensor able to overcome the lack of specificity usually attributed to laccase [29].

3.3 Calibration curves

In order to determine the calibration curves of our biosensor by means of time course measurements, Figs. 4a,b,c are used to single out the wavelength of the maximum in the absorption spectra of reaction products. As previously said, the absorption of either free or immobilized laccase at an optimized fixed wavelength (λ_{max} = 425 nm for hydroquinone, λ_{max} = 375 nm for resorcinol, λ_{nax} = 400 nm for catechol) is preliminarily measured and constitutes the baseline for the subsequent measurements. After addition of few μliters of solution of different phenols at various concentrations the time course of the absorption intensity is monitored and absorption changes for unit of time are determined. As an example in Fig. 5 the time changes (time course) in the absorption at the above-mentioned wavelength are monitored for a laccase solution (concentration equal to 1 mg/mL in 0.1 M acetate buffer pH 5) after addition of 0.4 mM of different phenols (*a* line for hydroquinone, *b* line for resorcinol and *c* line for catechol). As is evident the most significant changes occur for catechol conversely for hydroquinone and resorcinol enzymatic reaction shows less evident increases.

By performing time course measurements the analytical parameter defined as the absorption changes for unit of time A (min^{-1}) can be obtained by the following expression:

$$A = \frac{Abs^{\lambda max}(t) - Abs^{\lambda max}(t_0)}{t - t_0} \qquad (2)$$

where $Abs^{\lambda max}(t)$ is the absorption at the optimized fixed wavelength at *t* time and t_0 is the initial one. The values of A parameter are then determined for different analyte concentrations and linear calibration curves are obtained.

In Fig. 6a, the values of A from absorption time course of free laccase are reported as a function of hydroquinone concentration. The data show a Michaelis–Menten-type behaviour and are fitted by the following equation:

$$A = \frac{A_{\max} C}{K_m + C} \qquad 3)$$

where A_{max} is the saturation value of the absorption changes for unit of time, *C* in the analyte concentration and K_m is the apparent Michaelis–Menten constant.

The plot of the linear range is also reported in the inset of Fig. 6a and Hanes plot (not shown) allowed us to determine the A_{max} and K_m reported in Table 3. Similar results are obtained for resorcinol (Fig. 6b) and catechol (Fig. 6c), also in these cases the data follow a Michealis-Menten-type behaviour and the related parameters are reported in Table 3. From the K_m data of this Table it is possible to note that the highest affinity is shown by catechol while the lowest one is shown by resorcinol. The A_{max} values indicate that the laccase-phenols interactions are characterized by different reaction rates. In particular, the laccase-catechol interaction process has the highest reaction rates, while laccase-hydroquinone reaction confirms a very slow reaction rate [47, 48]. As far as concerns the other characteristics reported in Table 3, it is possible to note that largest linear range is obtained for resorcinol, while the best sensitivity and LOD are obtained for catechol. The LOD is calculated as signal-to-noise ratio equal 3. Given the very slow reaction rate of hydroquinone, the working characteristics of our laccase biosensor have been evaluated using resorcinol and catechol. The calibration curves for these two phenol compounds are reported in Figs. 7a and 7b together with related linear range plot and the kinetic parameters are also shown in Table 3. From this Table it can be noted that for catechol the immobilization procedure decreases the affinity, the reaction rate and the sensitivity, leaves unchanged the linear range and increases the LOD value. As far as concerns resorcinol the effects of immobilization are a decrease in affinity, an enlargement of linear range, a higher LOD value and an increase in reaction rate and sensitivity. This behaviour could be ascribed to some peculiar characteristic of the laccase-resorcinol interaction process, not yet well-described in literature or to some interaction between resorcinol and sol-gel matrix. It's important to note that no data on the use of laccase for resorcinol biosensing applications have been reported in literature to our knowledge. For this reason in Table 4 we report working parameters of biosensors prepared with laccase from *Trametes versicolor* only for catechol and hydroquinone. From the information reported in this Table it is possible to notice that the entrapment is the most used immobilization method even though also enzyme in solution is proposed for biosensing. Different values for the linear ranges and LOD are reported for the various kinds of biodevices. A time stability of 2 months is obtained for optical biosensor based on hybrid nafion/sol-gel silicate film [23] and for the amperometric biosensors using screen-printed

electrode [53]. It must be noted that also our sol-gel based biosensors shows a similar stability as above-reported (see also Ref. 33 for further information). From a comparison between Tables 3 and 4 it is evident that our biosensor shows valuable working features in comparison to other optical and amperometric catechol biosensing devices. In particular, the comparison with the other two optical biosensors reported in literature for catechol shows that the one based on hybrid nafion/sol-gel silicate film [23] has a compatible linear range but a worse LOD. For the biosensor reported in ref. 21 the linear range is significantly smaller and the LOD is better, but the above-mentioned biosensors are based on enzyme in solution that doesn't allow the reuse of enzyme.

As far as concerns hydroquinone concentration determination other attempts are underway to improve the kinetic of reaction with laccase by using additional agents [47] or nanomaterials and quantum dots [55, 56].

3.4 Recovery test with spiked samples

The analytical application of the proposed biosensor has been investigated by spiking water samples with 5 μM or 10 μM catechol or with 10 μM or 15 μM resorcinol. The recoveries have been in the range of 93-112% as reported in Table 5. These results confirm that the proposed method is useful for catechol and resorcinol determination in real samples.

4. Conclusions

In the present paper, a new sol-gel based optical biosensor for detection of different phenols compounds (catechol, resorcinol and hydroquinone) has been presented. Laccase from *Trametes versicolor* has been immobilized in an optically transparent sol-gel matrix and the catalytic elements characterized by FTIR spectroscopy. Using changes in the absorption of reaction products the concentration of the different analytes has been determined. Significant working parameters have been obtained for resorcinol and catechol. The case of resorcinol is particularly valuable since no other laccase based biosensors are reported in literature to our knowledge. The developed biosensor has been also successfully tested with real samples using tap water spiked with known amount of catechol and resorcinol.

The results here reported confirm that sol-gel immobilized laccase matrices can be used for constructing inexpensive and easy-to-use biosensors similar to the prototype described in one of our previous papers for glucose oxidase enzyme [33]. Moreover, the catalytic matrices can be also integrated into multi-microwell plates for a parallel and simultaneous detection of various samples [57]. It is important to note that the proposed biosensor exploits the intrinsic absorption spectra shown by laccase interacting with phenols without the use of other components. As say before the different characteristics of the above-mentioned spectra can contribute to improve the specificity of biosensors. For example, a step in this direction could be done by constructing complete calibration curves by monitoring the entire absorption spectra while the enzymatic reaction progresses in the presence of known amounts of various phenols. In such a way the determination of different phenols contemporarily present could be obtained [58] .

Acknowledgements

The authors are pleased to thank C. Camerlingo and I. Delfino for data wavelet analysis and useful discussions.

Conflict of interest The authors declare that they have no conflict of interest.

References

[1] Santodonato, B.R.M., and Neal, J.N.W. (1987) Toxicol. Ind. Health 3, 535-568.

[2] Rogers, K.R., Becker, R.K.R., Cembrano, J., and Chough, S.H. (2001) Talanta 54, 1059–1065.

[3] Thurston, C.F. (1994) Microbiology 140, 19-26.
[4]Fernández-Fernández, M., Sanromán, M.Á., and Moldes, D. (2013) Biotechnology Advances 31, 1808–1825.
[5] Claus, H. (2004) Micron 35, 93–96.
[6] Delfino, I., Viola, D., Cerullo, G., and Lepore, M. (2015) Biophysical Chemistry 200-201, 41–47.
[7] Bollag, J.M., Shuttleworth, K.L., and Anderson, D.H. (1988) Appl. Environ. Microbiol. 54, 3086-3091.
[8] Gupta, G., Rajendran, V., and Atanassov, P. (2003) Electroanalysis 15, 1577-1583.
[9] Gomes, S.A.S.S., and Rebelo, M.J.F. (2003) Sensor 3, 166-175.
[10] Haghighi, B., Rahmati-Panah, A., Shleev, S. and Gorton, L. (2007) Electroanalysis 19, 907–917.
[11] Casero, E., Petit-Domínguez, M.D., Vázquez, L., Ramírez-Asperilla, I., Parra-Alfambra, A.M., Pariente, F., and Lorenzo, E. (2013) Talanta 115, 401–408.
[12] Jędrychowska, A., Malecha, K., Cabaj, J., and Sołoducho, J. (2015) Electrochimica Acta 165, 372–382.
[13] Nazari, M., Kashanian, S., and Rafipour, R. (2015) Spectrochimica Acta Part A: Molecular and Biomolecular Spectroscopy 145, 130–138.

[14] Portaccio, M., Di Martino, S., Maiuri, P., Durante, D., De Luca, P., Lepore, M., Bencivenga, U., Rossi, S., De Maio, A., and Mita D.G. (2006) J. Mol. Catal. B: Enzymatic 41, 97-102.
[15] Portaccio, M., Di Tuoro, D., Arduini, F., Moscone, D., Cammarota, M., Mita, D.G., and Lepore, M. (2013) Electrochimica Acta 109, 340-347.
[16] Goldberg, M., and Pecht, I. (1974) Proc. Nat. Acad. Sci. USA 71, 4684-4687.

[17] Wynn, R.M., Sarkar, H.K., Holwerda, R.A., and Knaff, D.B. (1983) FEBS Letters 156, 23–28.

[18] Shleev, S.V., Morozova, O.V., Nikitina, O.V., Gorshina, E.S., Rusinova, T.V., Serezhenkov, V.A., Burbaev, D.S., Gazaryan, I.G., and Yaropolov, A.I. (2004) Biochimie 86, 693–703.
[19] Delfino, I., Portaccio, M., Della Ventura, B., Manzo, G., Mita, D.G., and Lepore, M. (2012) Proc. of SPIE 8439, 84391X-1.
[20] Rodriguez-Delgado, M.M., Aleman-Nava, G.S., Rodriguez-Delgado, J.M., Dieck-Assad, G., Martinez-Chapa, S.O., Barcelo, D., and Parra, R. (2015) Trends Anal. Chem 74, 21-45.

[21] Andreu-Navarro, A., Fernández-Romero, J.M., and Gómez-Hens, A. (2012) Analytica Chimica Acta 713, 1– 6.
[22] Godoy-Navajas, J., Paz Aguilar-Caballos, M., and Gómez-Hens, A. (2015) Food Chemistry 166, 29–34.
[23] Abdullah, J., Ahmad, M., Heng, L.Y., Karuppiah, N., and Sidek, H. (2007) Sensors 7, 2238–2250.
[24] Sanz, J., de Marcos, D., and Galban, (2012) J. Anal. Bioanl. Chem. 404, 351-359.
[25] Yaropolov, A.I., Kharybin, A.N. Emneus, J., Marko-Varga, G., and Gorton, L. (1995) Anal. Chim. Acta 308, 137-144.
[26] Zuyun, H., Houping, H., Ruxiu, C., and Yun'e, Z. (1998) Anal. Chim. Acta 374, 99–103.
[27] Cantarella, G., d'Acunzo, F., and Galli, C. (2003) Biotechnology and Bioengineering 82, 395-398.
[28] Moshtaghioun, S.M., Haghbeen, K., Sahebghadam, A.L., Legge, R.L., Khoshneviszadeh, R., and Farhadi, S. (2011) Anal. Chem. 83, 4200–4205.
[29] Xu, F. (1996) Biochemistry 35, 7608–7614.
[30] Brinker, J., and Scherer, G.W. (1990) The physics and chemistry of sol gel processing. Academic Press, New York.
[31] Jin, W., and Brennan, J.D. (2002) Anal. Chim. Acta 461, 1-36.
[32] Simkus, R.A., Laurinavicius, V., Boguslavsky, L., Skotheim, T., Tanenbaum, S.W., Nakasc, J.P., and Slomczynskic, D.J. (1996) Analytical Letters 29, 1907-1919.
[33] Portaccio, M., Lepore, M., Della Ventura, B., and Mita, D.G. (2009) J. Sol- Gel Sci. Technol. 50, 437-448.
[34] Portaccio, M., Della Ventura, B., Mita, D.G., Manolova, N., Stoilova, O., Rashkov, I., and Lepore, M. (2011) J. Solgel Sci. Technol. 57, 204–211.
[35] Delfino, I., Portaccio, M., Della Ventura, B., Mita, D.G., and Lepore, M. (2013) Mater. Sci. Eng. C 33, 304–310.
[36] Reetz, M.T. (1997) Adv. Mater. 9, 943–954.
[37] Camerlingo, C., Zenone, F., Gaeta, G.M., Riccio, R., and Lepore, M. (2006) Meas. Sci. Technol. 17, 298-303.
[38] Barth, A. (2007) Biochim. Biophys. Acta 1767, 1073-1101.

[39] Nocun, M., Leja, E., Jedlinski, L., and Najman, J. (2005) J. Mol. Struct. 744–747, 597-602.
[40] Coates, J. (2000) Interpretation of infrared spectra: A practical approach, J. Wiley and Sons Ltd, Chichester.
[41] Cicco, N., Morone, A., Verrastro, M., Dinescu, M., Matei, A., Mitu, B., and Centone, D. (2015) Sensors Lecture Notes in Electrical Engineering 319, 47-51.
[42] Camacho CórdovaI, D.I., Morales Borgesi, R., Carbajal Arizaga, G.G., Wypych, F. and N. Krieger, (2009) Quim. Nova 32, 1495-1499.
[43] El-Batal, A.I., ElKenawya, N.M., Yassin, A.S., Amin, M.A. (2015) Biotechnology Reports 5, 31–39.
[44] Diaconu, M., Litescu, S.C., Radu, G.L. (2010) Sensors and Actuators B 145, 800–806.
[45] Revina, A.A., Khaikin, G.L., Protasova, E.L., Mezentseva, N.B., Stepanova, E.V., and Skorobogat'co, O.V. (2000) Russ.Chem.Bull. Int. Ed 49, 1464-1467.
[46] Shimomura, T., Itoh, T., Sumiya, T., Hanaoka, T., Mizukamia, F., and Ono, M. (2011) Sensors and Actuators B 153, 361–368.
[47] Holwerda, R.A., and Gray, H.B. (1974) J. Am. Chem. Soc. 96, 6008-6022.
[48] Sirajuddin, M.I., Bhanger, A., Niaz, A., Shah, A., and Rauf, A. (2007) Talanta 72, 546–553.
[49] Sondhi, S., Sharma, P., Saini, S., Puri, N., and Gupta, N. PLoS ONE 9(5): e96951. doi:10.1371/journal.pone.0096951.
[50] Duncan, W.R., and Prezhdo, O.V. (2005) J. Phys. Chem. B 109, 365-373.
[51] Aronica, C., Venancio-Marques, A., Chauvin, J., Robert, V., and Lemercier, G. (2009) Chem. Eur. J. 15, 5047–5055.
[52] Xu, X., Lu, P., Zhou, Y., Zhao, Z., and Guo, M. (2009) Mater.Sci.Eng. C 29, 2160–2164.
[53] Ibarra-Escutia, P., Juarez-Gómez, J., Calas-Blanchard, C., Marty, J.L., and Ramírez-Silva, M.T. (2010) Talanta 81, 1636–1642.
[54] Haghighi, B., Gorton, L., Ruzgas, T., and Jönsson, L.J. (2003) Anal.Chim.Acta 487, 3–14.
[55] Upan, J., Reanpang, P., Chailapakul, O., and Jakmunee, J. (2016) Talanta 146, 766-771.
[56] Akshath, U.S., Shubha, L.R., Bhatt, P., and Thakur, M. S. (2014) Biosensors and Bioelectronics 57, 317–323.
[57] Schäferling, M., Wu, M., and Wolfbeis, O.S. (2004) J.Fluorescence 14, 561-568.
[58] De Luca, M., Oliverio, F., Ioele, G., and Ragno, G. (2009) Chemometrics and Intelligent Laboratory Systems 96, 14–21.

FIGURE CAPTIONS

Figure 1 – A representative scheme of catalytic sol-gel matrix preparation process.

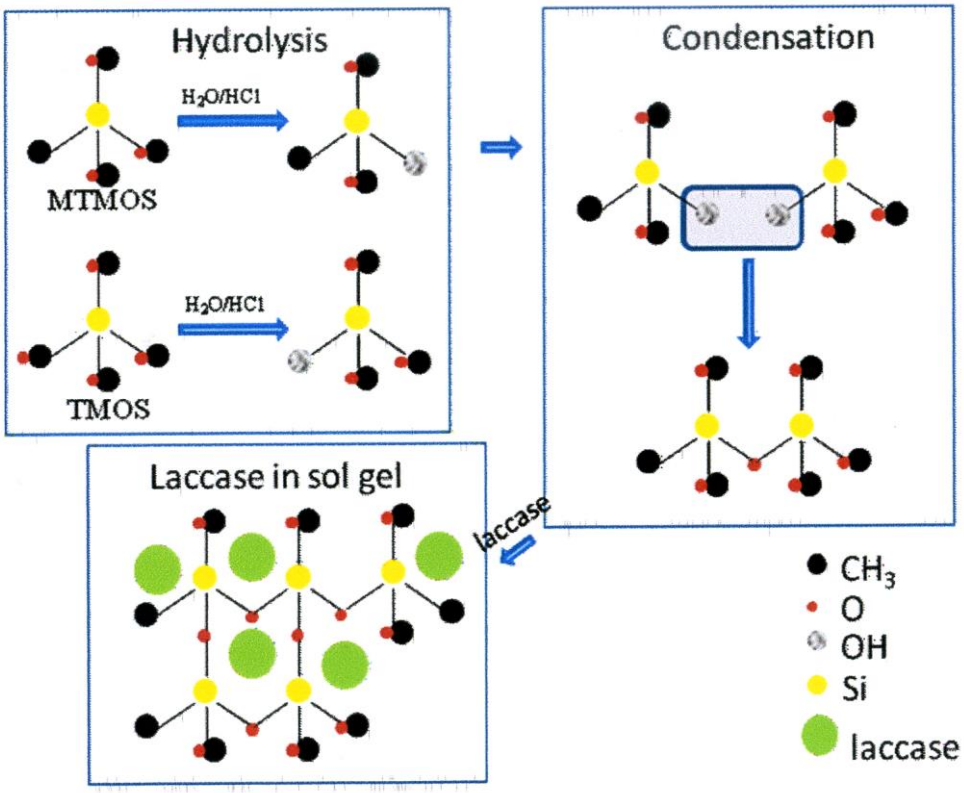

Figure 2 – a) FT-IR spectrum of a laccase powder sample; b) FT-IR spectrum of a bare sol-gel sample (dashed line) and a sample of laccase immobilized in sol-gel (continuous line). In the inset a selected region of the spectrum of immobilized laccase after subtraction of sol-gel contribution using wavelet procedure.

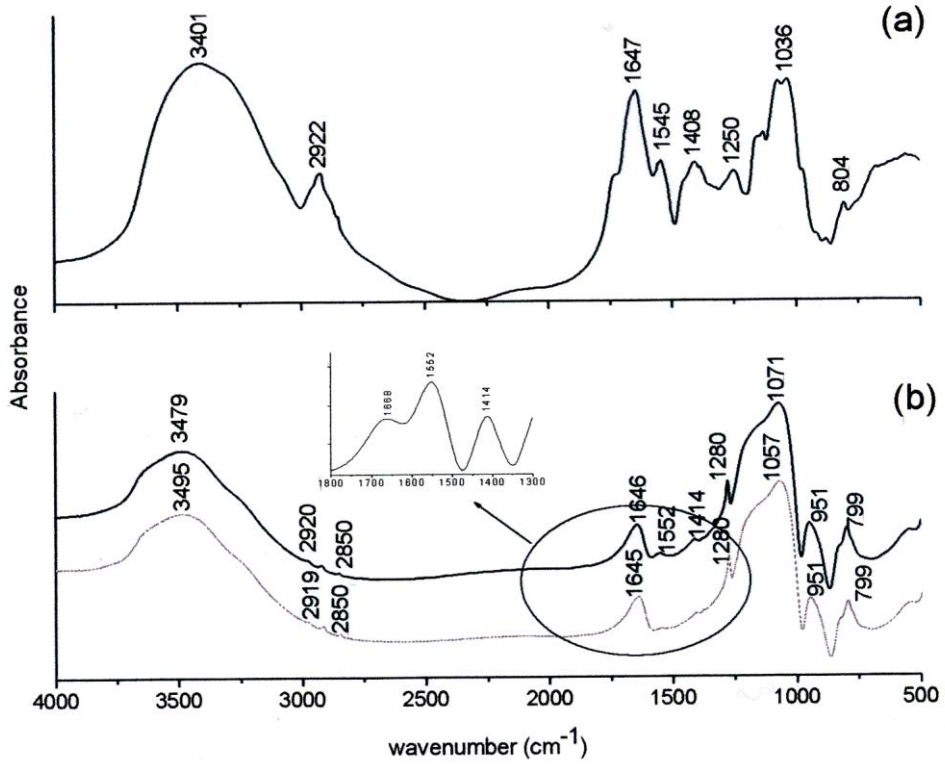

Figure 3 – (a) Absorption spectrum of free laccase solution (concentration 1mg/mL in 0.1 M acetate buffer at pH = 6.5). In the inset the region 400-900 nm is reported; - (b) Absorption spectra of laccase immobilized in sol-gel matrix (i) and of a bare sol-gel sample (ii).

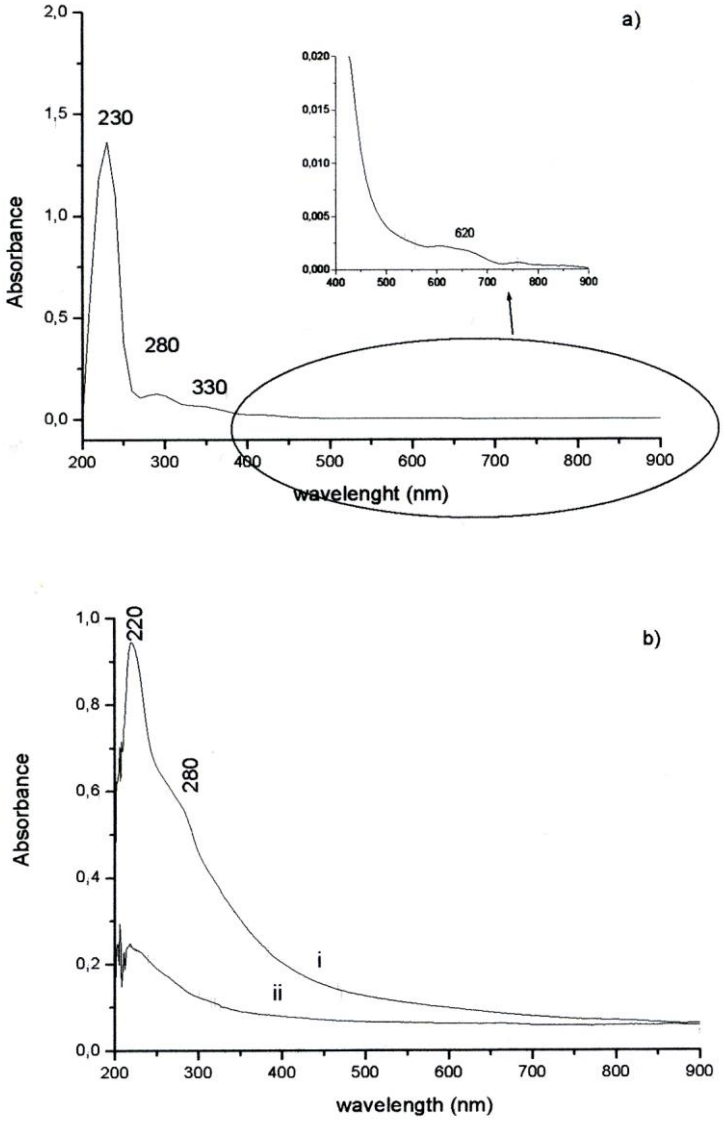

Figure 4 – (a) Absorption spectra of hydroquinone (dashed line) and laccase-reaction product (continuous line); (b) the same for resorcinol; (c) the same for catechol. In the inset the spectra in the range 300-600 nm. Experimental conditions: [hydroquinone] = [resorcinol] = [catechol] = 0.4 mM and [laccase] = 8 μg/mL in 0.1 M acetate buffer at pH = 5.

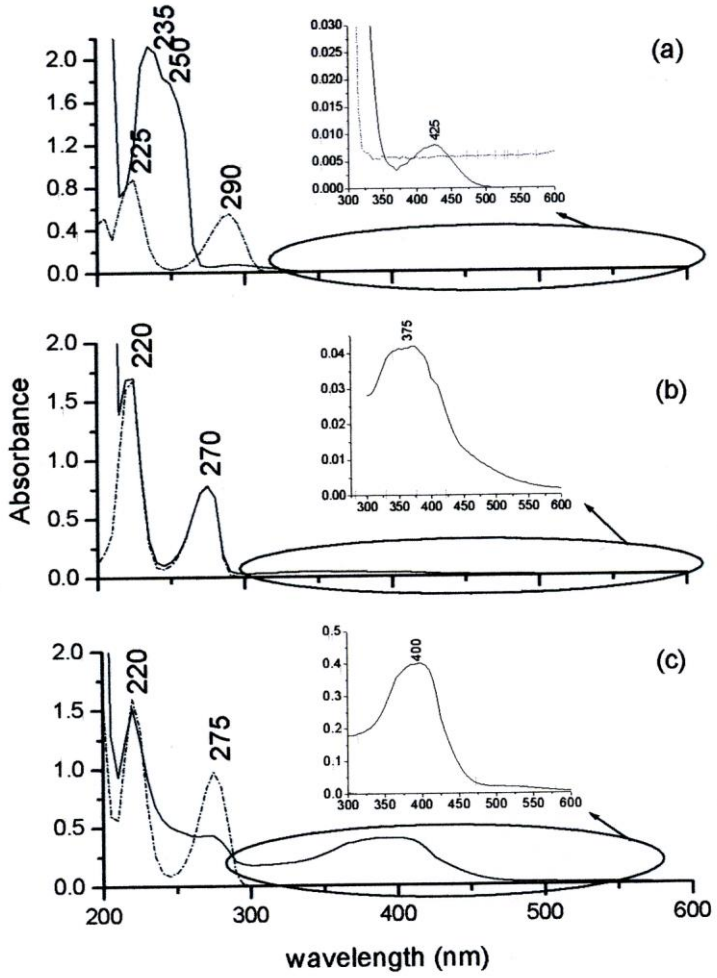

Figure 5 – Time course behaviour of absorbance values for the three different aromatic compounds oxidation catalyzed by laccase, in the experimental conditions of Figs. 4a, 4b and 4c .

a) hydroquinone, b) resorcinol, c) catechol.

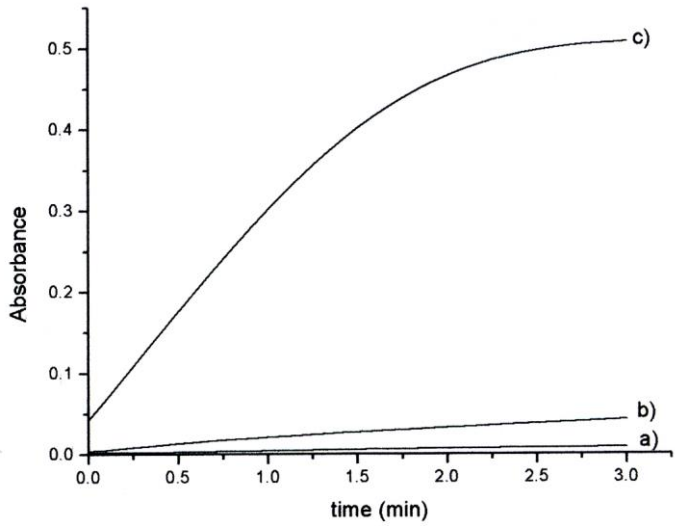

Figure 6 – Calibration curve of free laccase as a function of substrate concentration obtained by monitoring absorption at : (a) 425 nm for hydroquinone; (b) 375 nm for resorcinol; (c) 400 nm for catechol. In the inset the linear range for biosensor response. Experimental conditions: [hydroquinone] = [resorcinol] = [catechol] = 0.4 mM and [laccase] = 8 μg/mL in 0.1 M acetate buffer at pH = 5.

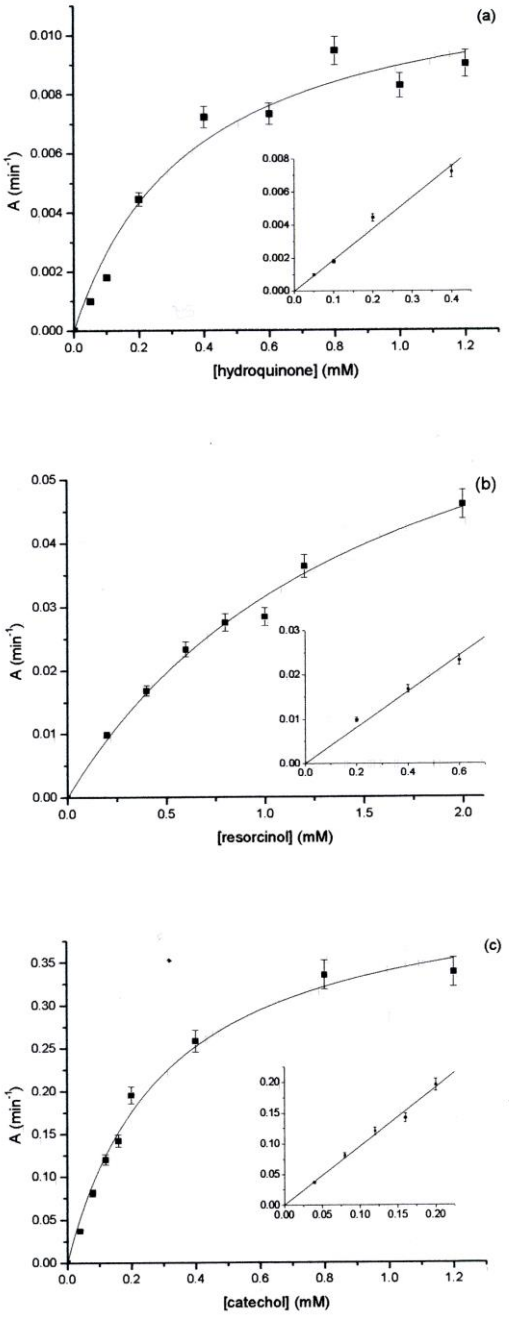

Figure 7 – Calibration curve of laccase in sol-gel matrix as a function of substrate concentration obtained by monitoring absorption at : (a) 375 nm for resorcinol; (b) 400 nm for catechol. In the inset the linear range for biosensor response. Experimental conditions: resorcinol an catechol in 0.1 M acetate buffer at pH = 5

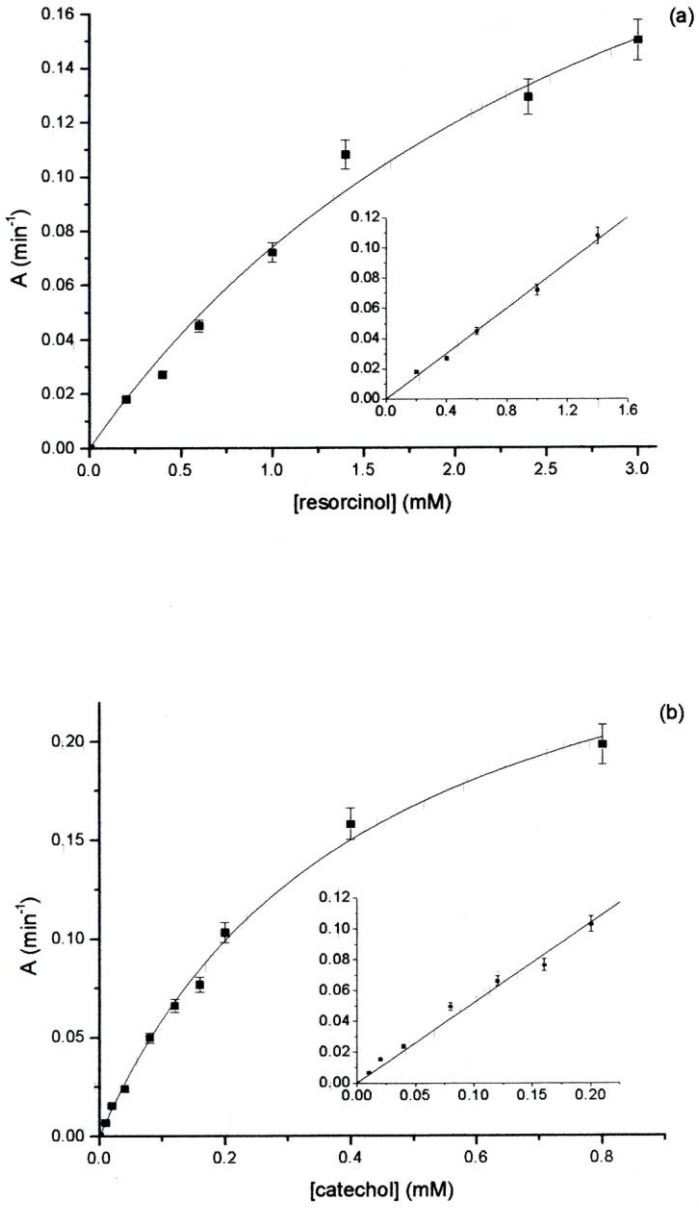

TABLE CAPTIONS

Table 1 Main peaks in the FT-IR spectrum of free laccase sample and tentative assignment according to refs. [34, 38]

Table 2 Main peaks in the FT-IR spectrum of sol–gel sample and tentative assignment according to refs. [34, 38-40]

Table 3 Optokinetic parameters from calibration curves analysis for laccase in solution and immobilized (where LOD is defined as three times the signal-to-noise ratio).

Table 4 Working parameters of some *Trametes versicolor* laccase-based biosensors as reported in literature (n.a. stands for not available)

Table 5 Recovery studies of spiked tap water samples. The measurements were performed in triplicate and the evaluated parameters are expressed as the mean of the three replicates $\pm$ SD.

TABLE 1

Wavenumber (cm^{-1})	Assignments
3401	amide A; O-H stretching
2922	CH symmetric stretching in CH_2
1647	C=O stretching amide I
1545	N–H bending amide II
1408	C–H bending CH_3
1250	amide III
1036	C–O stretching
804	amide V

TABLE 2

Wavenumber (cm^{-1})	Assignments
3495	H-bonded silanol ; O–H stretching
2919	CH asymmetric stretching in O–CH_3
2850	CH symmetric stretching in O–CH3
1645	H-bonded silanol and adsorbed water O–H bending
1280	Si-CH_3, symmetric CH_3 deformation vibration
1057	Si–O–Si asymmetric stretching
951	Si–OH deformation vibration
799	Si–O–Si Symmetric stretching

TABLE 3

Laccase form	**Phenol compound**	**K_m** (mM)	**A_{max}** (min^{-1})	**Linear Range** ($10^{3}\mu M$)	**Sensitivity** (min^{-1} mM^{-1})	**LOD (μM)**
Enzyme in solution	hydroquinone	0.362 ± 0.095	0.012 ± 0.001	up to 0.4	0.019 ± 0.001	6
Enzyme in solution	resorcinol	1.587 ± 0.267	0.081 ± 0.008	up to 0.6	0.040 ± 0.001	3
Enzyme in solution	catechol	0.306 ± 0.038	0.444 ± 0.022	up to 0.2	0.957 ± 0.020	0.1
Enzyme in sol-gel	resorcinol	3.232 ± 0.844	0.313 ± 0.051	up to 1.4	0.075 ± 0.001	4.5
Enzyme in sol-gel	catechol	0.424± 0.040	0.309 ± 0.015	up to 0.2	0.521 ± 0.016	0.6

TABLE 4

Immobilization support and method	Substrate	Linear range (μM)	LOD (μM)	Stability	Refs
Optical biosensor based on hybrid nafion/sol-gel silicate film *Crosslinking + entrapment*	Catechol	500 - 800	330	2 months	[23]
Optical biosensor based on enzyme in solution	Catechol	0.08–5	0.01		[21]
Amperometric biosensor based on modified mesoporous silica MCM-41/PVA *Entrapment*	Catechol	4.0–87.98	0.331	n.a.	[52]
Optical biosensor based on enzyme in solution	Hydroquinone	0.05–2	0.01		[21]
Amperometric biosensor based on a high resolution photopolymer deposited onto a screen-printed electrode *Entrapment*	Hydroquinone	1.1–130	1.07	2 months	[53]
Amperometric biosensor based on graphite electrodes *Adsorption*	Hydroquinone	0.5–8	0.44	Some days	[54]

TABLE 5

Sample	contaminant added	Concentration added (μM)	Concentration found (μM)	Recovery (%)
1	catechol	5.0	5.6 ± 0.3	112 ± 4
2	catechol	10	9.7± 0.5	97 ± 5
3	resorcinol	10	9.3 ± 0.5	93 ± 5
4	resorcinol	15	16.6 ± 0.8	111 ± 5